Synthesis and evaluation of (Z)-2,3-diphenylacrylonitrile analogs as anti-cancer and anti-microbial agents

ARTICLE *in* EUROPEAN JOURNAL OF MEDICINAL CHEMISTRY · SEPTEMBER 2013

Impact Factor: 3.45 · DOI: 10.1016/j.ejmech.2013.08.031 · Source: PubMed

3 AUTHORS, INCLUDING:

Mohammad Sayed Alam
Dongguk University
45 PUBLICATIONS **261** CITATIONS
SEE PROFILE

Lee Dong-Ung
Jagannath University - Bangladesh
74 PUBLICATIONS **1,042** CITATIONS
SEE PROFILE

European Journal of Medicinal Chemistry 69 (2013) 790–797

Contents lists available at ScienceDirect

European Journal of Medicinal Chemistry

journal homepage: http://www.elsevier.com/locate/ejmech

Original article

Synthesis and evaluation of (*Z*)-2,3-diphenylacrylonitrile analogs as anti-cancer and anti-microbial agents

Mohammad Sayed Alam [a], Young-Joo Nam [b], Dong-Ung Lee [b, *]

[a] *Department of Chemistry, Jagannath Univeristy, Dhaka 1100, Bangladesh*
[b] *Division of Bioscience, Dongguk University, Gyeongju 780-714, Republic of Korea*

ARTICLE INFO

Article history:
Received 30 March 2013
Received in revised form
25 August 2013
Accepted 31 August 2013
Available online 19 September 2013

Keywords:
Acrylonitriles
Cytotoxicity
Antimicrobial activity
Human cancer cell line

ABSTRACT

In the present study, a series of (*Z*)-2,3-diphenylacrylonitrile analogs were synthesized and then evaluated in terms of their cytotoxic activities against four human cancer cell lines, *e.g.* lung cancer (A549), ovarian cancer (SK-OV-3), skin cancer (SK-MEL-2), and colon cancer (HCT15), as well as anti-microbial activities against three microbes, *e.g. Staphylococcus aureus*, *Salmonella typhi*, and *Aspergillus niger*. The title compounds were synthesized by Knoevenagel condensation reaction of benzyl cyanide or *p*-nitrobenzyl cyanide with substituted benzaldehydes in good yields. Most of the compounds exhibited significant suppressive activities against the growth of all cancer cell lines. Compound **3c** was most active in inhibiting the growth of A549, SK-OV-3, SK-MEL-2, and HCT15 cells lines with IC_{50} values of 0.57, 0.14, 0.65, and 0.34 mg/mL, respectively, followed by compounds **3f**, **3i**, and **3h**. Compound **3c** exhibited 2.4 times greater cytotoxic activity against HCT15 cells, whereas it showed similar potency against SK-OV-3 cells to that of the standard anti-cancer agent doxorubicin. Structure–activity relationship study revealed that electron-donating groups at the *para*-position of phenyl ring B were more favorable for improved cytotoxic activity, whereas the presence of electron-withdrawing groups was unfavorable compare to unsubstituted acrylonitrile. An optimal electron density on phenyl ring A of (*Z*)-2,3-diphenylacrylonitrile analogs was crucial for their cytotoxic activities against human cancer cell lines used in the present study. Qualitative structure–cytotoxic activity relationships were studied using physicochemical parameters; a good correlation between calculated polar surface area (PSA), a lipophobic parameter, and cytotoxic activity was found. Moreover, all compounds showed significant anti-bacterial activities against *S. typhi*, whereas compound **3k** showed potent inhibition against both *S. aureus* and *S. typhi* bacterial strains.

1. Introduction

A number of acrylonitrile analogs with a wide range of interesting biological activities have been reported. For example, Tagmose and co-workers have described the synthesis and biological evaluation of 3,3-diamino-sulfonylacrylonitriles as novel inhibitors of glucose-induced insulin secretion from beta cells [1]. Carta and co-workers have reported the synthesis of 3-aryl-2-(1H-benzotriazol-1-yl)acrylonitrile analogs along with their anti-bacterial, anti-fungal, anti-mycobacterial, anti-retroviral, and anti-tumor activities [2–4]. Further, Sączewski et al. [5,6] have reported the synthesis, cytotoxic and antibacterial activities of novel 2,3- and 2,6-disubstituted heteroarylacrylonitriles. Recently, Hranjec and co-workers reported the synthesis and *in vitro* antitumor evaluation of benzimidazolyl 2,3-disubstituted acrylonitriles [7]. More recently, Zificsak and co-workers reported the synthesis of sulfonyl acrylonitrile derivatives and their biological evaluation as novel inhibitors of peritoneal carcinomatosis [8].

Resveratrol (Fig. 1), a naturally occurring hydroxylated stilbene analog, which has been found in many medicinal plants, grape skin, peanuts, and red wine [9], shows potent chemopreventive activity [10] by exerting anti-proliferative and pro-apoptotic effects in human cancer cells [11]. Recently, a good number of stilbene analogs has been isolated as well as synthesized from natural sources, displaying a wide range of interesting biological activities [12–16]. Polyhydroxy stilbenes possesses strong anti-oxidative [17] and anti-inflammatory [18] activities that lead to chemotherapeutic properties such as anti-cancer-promoting activity. Resveratrol, a polyhydroxylated stilbene analog, exerts its anti-cancer activity by triggering the synthesis of endogenous ceramide [19,20], a bioactive sphingolipid [21,22]. Ceramide is a promising pharmacological target when either major apoptotic pathway is disrupted or resistance to DNA damage elevated. Moreover, drugs that trigger ceramide, while highly effective in malignant cells, are less toxic to

* Corresponding author. Tel.: +82 54 770 2224; fax: +82 54 742 9833.
E-mail address: dulee@dongguk.ac.kr (D.-U. Lee).

0223-5234/$ – see front matter © 2013 Elsevier Masson SAS. All rights reserved.
http://dx.doi.org/10.1016/j.ejmech.2013.08.031

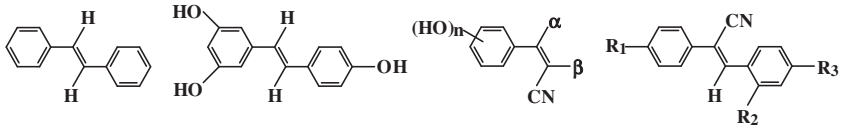

(*E*)-Stilbene (*E*)-Resveratrol Tyrphostins (*Z*)-Diphenylacrylonitriles

Fig. 1. Structures of key molecules.

normal cells and tissues [23]. Resveratrol and its analog have been reported as apoptosis-inducing agents, aryl hydrocarbon receptor (AhR) modulators, and human cytochrome P450 (CYP) inhibitors, specifically as selective inhibitors of the isoform CYP1B1 [24–26]. Tyrphostins (tyrosine phosporylation inhibitors), hydroxylated styrenes (Fig. 1), are used as potential protein tyrosine kinase inhibitors [27]. Protein tyrosine kinase plays an important role in normal cell division and abnormal cell proliferation, its enhanced activity is considered to be related with proliferative diseases such as cancer. In addition, several kinds of tyrphostin derivatives such as substituted quinazoline-tyrphostins [28] and modified phenolic tyrphostins [29] exerted anticancer properties against human cancer cell lines.

Due to our ongoing interest in identifying novel biologically active molecules, we have designed and synthesized (*Z*)-2,3-diphlenylacrylonitriles, which are structurally similar to resveratrol, a *trans*-stilbene analog and tyrphostins. The syntheses of (*Z*)-2,3-diphenylacrylonitrile analogs were carried out by a simple but efficient Knoevenagel condensation reaction of benzyl cyanide or substituted benzyl cyanide with various substituted benzaldehydes in ethanol. Structures of the new compounds were elucidated by IR, ^{1}H NMR, and elemental analyses. We investigated the *in vitro* cytotoxic activities of these new compounds against four culture cell lines, *e.g.* A549 (human lung cancer), SK-OV-3 (human ovarian cancer), SK-MEL-2 (human skin cancer), and HCT15 (human colon cancer). Physicochemical calculations were also carried out in order to determine the relationship between the electronic properties and cytotoxic activities of (*Z*)-2,3-diphenylacrylonitrile analogs. Furthermore, *in vitro* anti-microbial activities were screened against two bacterial strains and one fungal strain, *e.g. Staphylococcus aureus*, *Salmonella typhi*, and *Aspergillus niger*.

2. Results and discussion

2.1. Chemistry

The desired compounds **3a**–**r** were synthesized according to a convenient one-step reaction depicted in Scheme 1, by Knoevenagel condensation of the appropriate benzyl cyanide or *p*-nitrobenzyl cyanide with the suitable substituted benzaldehyde in ethanol, using sodium ethoxide as basic catalyst. All compounds except **3a**, **3b**, and **3i** are new. The structures of the compounds were assigned by IR, ^{1}H NMR, and elemental analyses. In the IR spectra of the compounds, characteristic –C≡N stretching absorption bands appeared around 2190–2230 cm^{-1}. Although two geometric isomers were obtained in the Knoevenagel condensation, we observed that in all cases, the *Z*-isomer was the only product supported by the proton NMR spectra. From the literature survey, it has been found that the vinylic-H of *E*-isomers exhibits a down-field shift (δ 8.81–7.65) compared to that of *Z*-isomers (δ 7.60–6.03) [3,4,30]. In the ^{1}H NMR spectra, the vinylic proton (–CH=C–) of all compounds appeared at 6.96–7.52 ppm as a broad singlet equivalent to one proton, and at higher field compared to that of *E*-isomer, which supported the *Z*-configuration of all compounds. The aromatic protons were assigned in the usual manner, according to their substitution pattern. The methoxy protons of compounds **3b** and **3k** appeared as singlets at 3.87 and 3.89 ppm, respectively. The methyl protons of compounds **3i** and **3r** were observed as singlets at 2.41 and 2.42 ppm, respectively, equivalent to three protons each. The *N,N′*-dimethyl protons of compounds **3c** and **3l** were observed as singlets at 2.91 and 2.89 ppm, respectively, equivalent to six protons each.

2.2. Cytotoxic activity

The cytotoxic activities of (*Z*)-2,3-diphenylacrylonitrile analogs (**3a**–**r**) were evaluated by an *in vitro* assay performed on four human cancer cell lines, *e.g.* lung cancer (A549), ovarian cancer (SK-OV-3), skin cancer (SK-MEL-2), and colon cancer (HCT15). Their cytotoxic activities were evaluated by measuring the inhibition of net cell growth, as measured as a percentage of the control samples, after incubation for 48 h with the test samples following the SRB (sulforhodamine-B) method. All activities were compared with doxorubicin as a positive control. As observed in Table 1, compound **3c** showed the highest cytotoxic activity against all cancer cell lines, followed by compounds **3f**, **3i**, and **3h**. Compound **3c** exhibited 2.4 times greater cytotoxic activity against HCT15 cancer cells (IC_{50} 0.34 μg mL^{-1}), whereas it showed similar potency against SK-OV-3 cancel cells (IC_{50} 0.14 μg mL^{-1}) to that of the standard anti-cancer agent doxorubicin (IC_{50} 0.814 and 0.092 μg mL^{-1}, respectively). However, this compound displayed lower activity against other two cancer cell lines, A549 and SK-MEL-2.

Structure–activity relationship study revealed that the nature of the substituted group on the phenyl ring of (*Z*)-2,3-diphenylacrylonitriles plays an important role in the cytotoxic activity of the compound. Compound **3a**, which possessed two unsubstituted phenyl rings, showed greater cytotoxicity against SK-MEL-2 cells (IC_{50} 38.45 mg mL^{-1}) than against A549 (IC_{50} 43.76 mg mL^{-1}), SK-OV-3 (IC_{50} 47.39 mg mL^{-1}), and HCT15 (IC_{50} 68.98 mg mL^{-1}) cells. Introduction of a *N,N*-dimethylamino group, a stronger electron-donating group, at the *para*-position of phenyl ring B resulted in compound **3c**, which exhibited 76, 339, 59, and 203 times greater activities against A549 (IC_{50} 0.57 mg mL^{-1}), SK-OV-3 (IC_{50} 0.14 mg mL^{-1}), SK-MEL-2 (IC_{50} 0.65 mg mL^{-1}), and HCT15 (IC_{50} 0.34 mg mL^{-1}) cells, respectively, compared with those of **3a**. Further, introduction of a nitro group, a stronger electron-withdrawing group, at the *para*-position of phenyl ring A or B resulted in compounds **3e** and **3j**, respectively. The former compound showed similar cytotoxicities against SK-MEL-2 and SK-OV-3 cancer cells along with increased cytotoxicity against A549 and HCT15 cells compared with those of **3a**, whereas the latter

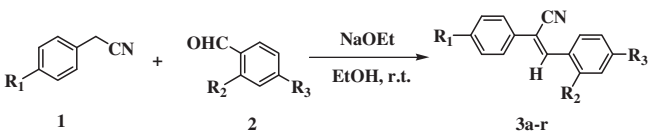

Scheme 1. Synthesis of (*Z*)-2,3-diphenylacrylonitrile analogs.

Table 1
In vitro cytotoxicity data of (Z)-2,3-diphenylacrylonitrile analogs (**3a**–**r**) against selected human cancer cell lines.

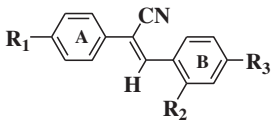

Comp	R_1	R_2	R_3	IC_{50} (μg mL^{-1})[a]			
				A549[b]	SK-OV-3[c]	SK-MEL-2[d]	HCT15[e]
3a	H	H	H	43.76	47.39	38.45	68.98
3b	H	H	OMe	25.51	14.93	25.17	23.16
3c	H	H	NMe_2	0.57	0.14	0.65	0.34
3d	H	NO_2	H	44.45	48.59	38.95	70.12
3e	H	H	NO_2	37.76	48.97	35.16	44.85
3f	H	H	Cl	1.81	0.20	1.53	1.22
3g	H	Cl	H	31.56	18.63	25.53	33.76
3h	H	H	Br	18.19	5.57	14.46	13.98
3i	H	H	CH_3	1.82	0.58	1.63	1.51
3j	NO_2	H	H	34.10	39.24	33.95	40.12
3k	NO_2	H	OMe	35.65	34.05	32.14	69.12
3l	NO_2	H	NMe_2	77.59	78.97	75.85	81.12
3m	NO_2	NO_2	H	72.35	74.90	52.65	>100.0
3n	NO_2	H	NO_2	32.95	35.85	37.50	39.86
3o	NO_2	H	Cl	82.96	85.30	83.43	83.06
3p	NO_2	Cl	H	17.86	7.27	16.14	88.90
3q	NO_2	H	Br	89.75	>100.0	69.76	92.65
3r	NO_2	H	CH_3	75.51	71.98	59.98	>100.0
Doxorubicin				0.011	0.092	0.009	0.814

[a] IC_{50} values were obtained using a dose response curve by nonlinear regression using a curve fitting program, OriginPro 7.5.
[b] Human lung cancer.
[c] Human ovarian cancer.
[d] Human skin cancer.
[e] Human colon cancer.

compound exhibited increased activities against all cancer cell lines. Introduction of a nitro group at the *ortho*-position instead of the *para*-position of phenyl ring B of **3a** yielded compound **3d,** which showed similar cytotoxicity as **3a**. On the other hand, compound **3d** showed significantly increased activities against A549, SK-MEL-2, and HCT15 cells as well as similar activity against SK-OV-3 cells compared with those of a *para*-nitro analog, compound **3e**. Introduction of a methyl group, a weak electron-donating group, at the *para*-position of phenyl ring B resulted in compound **3i**, which exhibited 24, 81, 23, and 45 times greater activities against A549 (IC_{50} 1.82 mg mL^{-1}), SK-OV-3 (IC_{50} 0.58 mg mL^{-1}), SK-MEL-2 (IC_{50} 1.63 mg mL^{-1}), and HCT15 (IC_{50} 1.51 mg mL^{-1}) cells, respectively, compared with those of **3a**. On the other hand, it showed 2.5–4.5 times lower cytotoxicities against all cancer cell lines compared to those of **3c**, a *N*,*N*-dimethylamino analog. Increasing the electron-donating capacity of the methyl group by replacement with a methoxy group (compound **3b**) led to a substantial (14–25 times) loss in activity, although compound **3b** showed significant increased cytotoxicities (1.7–3.2 times) against all cell lines compared with those of **3a**, an unsubstituted acrylonitrile. Compounds with halogen substituents (**3f** and **3h**) at the *para*-position of phenyl ring B, which showed weak electron-withdrawing capacity but also electron-donating ability due to the resonance effect, displayed significantly improved cytotoxicities against all cell lines compared to those of **3a**. Though the methoxy group has greater electron donating capacity than chlorine atom, compound **3b,** a *para*-methoxy analog showed less cytotoxicity against all cancer cell lines compared to that of **3f**, a *para*-chloro analog. Compound **3f**, with chlorine substituted at the *para*-position of phenyl ring B, showed 24, 237, 25, and 57 times greater

Table 2
Molinspiration calculations of molecular properties of compounds (**3a**–**r**).

Comp.	MW (g/mol)	cLogP[a]	TPSA[b]	OH–NH interact[c]	O–N interact[d]	nrotb[e]	Volume
3a	205.260	3.785	23.792	0	1	2	199.728
3b	235.286	3.842	33.026	0	2	3	225.274
3c	248.329	3.887	27.03	0	2	3	245.634
3d	250.257	3.516	69.616	0	4	3	223.063
3e	250.257	3.744	69.616	0	4	3	223.063
3f	239.705	4.463	23.792	0	1	2	213.264
3g	239.705	4.235	23.792	0	1	2	213.264
3h	284.156	4.594	23.792	0	1	2	217.614
3i	219.287	4.234	23.792	0	1	2	216.289
3j	250.257	3.744	69.616	0	4	3	223.063
3k	280.283	3.801	78.85	0	5	4	248.608
3l	293.326	3.846	72.854	0	5	4	268.968
3m	295.254	3.475	115.44	0	7	4	246.397
3n	295.254	3.703	115.44	0	7	4	246.397
3o	284.702	4.422	69.616	0	4	3	236.598
3p	284.702	4.194	69.616	0	4	3	236.598
3q	329.153	4.553	69.616	0	4	3	240.948
3r	264.284	4.193	69.616	0	4	3	239.624

[a] Calculated octanol/water partition coefficient.
[b] Molecular polar surface area.
[c] Number of hydrogen-bond donors.
[d] Number of hydrogen-bond acceptors.
[e] Number of rotatable bonds.

cytotoxicities against A549 (IC_{50} 1.81 mg mL^{-1}), SK-OV-3 (IC_{50} 0.20 mg mL^{-1}), SK-MEL-2 (IC_{50} 1.53 mg mL^{-1}), and HCT15 (IC_{50} 1.22 mg mL^{-1}) cells, respectively, compared with those of **3a**. Compound **3h**, with bromine substituted at the *para*-position of phenyl ring B, showed reduced activities (9–28 times) against all cancer cell lines compared with those of compound **3f**. Introduction of a chlorine atom at the *ortho*-position instead of *para*-position of phenyl ring B of **3a** yielded compound **3g**, which resulted in improved cytotoxicity compared with that of **3a** but dramatically reduced activities against all cancer cell lines compared with those of compound **3f**. On the other hand, introduction of a nitro group, a highly polar group, at the *para*-position of phenyl ring A of compounds **3b**–**i** yielded compounds **3k**–**r**. All of these compounds (**3k**–**m**, **3o**, **3q**, and **3r**) showed significantly reduced activities against all cancer cell lines except for compounds **3n** and **3p**. Compound **3n** showed significantly improved activities against A549, SK-OV-3, and HCT15 cell lines but reduced activity against SK-MEL-2 cells, whereas compound **3p** exhibited significantly improved activities against A549, SK-OV-3, and SK-MEL-2 cell lines but reduced activity against HCT15 cells compared to their corresponding compounds **3e** and **3g**, respectively. The above structure–activity relationships led us to hypothesize that an optimum electron density on phenyl ring B of (*Z*)-2,3-diphenylacrylonitriles may be closely related to maximum cytotoxic activity against the cell lines used in the present study. Further structure-activity studies with versatile analogs are needed to clearly elucidate the role of structure on the cytotoxicity of (*Z*)-2,3-diphenylacrylonitriles as well as to identify their molecular targets.

2.3. Computational studies

The physicochemical properties of a molecule play an important role in determining molecular reactivity in a biological response [31]. As biological systems are furnished with a number of heterogeneous phases, *e.g.* water, serum protein, lipid particles etc., drug transport processes and drug–receptor interactions are essentially physicochemical. Polar surface area (PSA) or lipophilicity is recognized as a meaningful parameter in structure–activity relationship studies and has become the single most informative and successful physicochemical property in medicinal

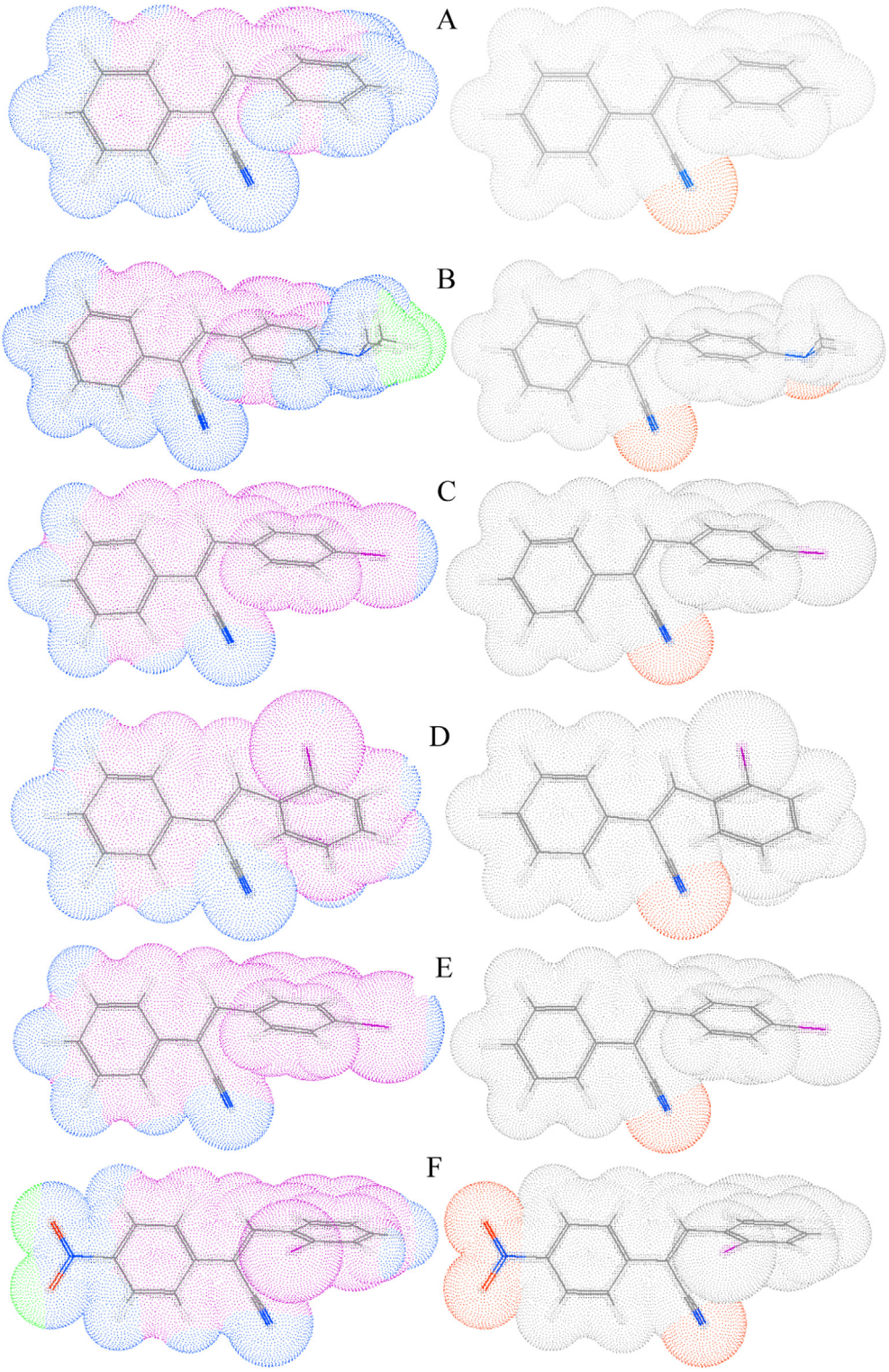

Fig. 2. Maps of lipophilicity potential (left) and polar surface area (right) of **3a** (A), **3c** (B), **3f** (C), **3g** (D), **3h** (E), and **3p** (F) showing the most lipophilic area (pink color), intermediate lipophilic area (green color), most hydrophobic area (blue color), nonpolar area (gray white color), and polar area (red color). (For interpretation of the references to color in this figure legend, the reader is referred to the web version of this article.)

chemistry [32]. Nowadays, it is recognized as a major experimental and theoretical tool in drug design.

To explain the qualitative structure-anti-cancer activity relationships (QSAR) of (*Z*)-2,3-diphenylacrylonitriles (**3a**–**r**), physicochemical calculations were carried out using molinspiration cheminformatics software. Physiochemical parameters of some selected (*Z*)-2,3-diphenylacrylonitrile analogs are listed in Table 2. The lipophilic character of a molecule depends on two important factors, *i.e.* hydrophobicity and polarity, which help the molecule to cross or irreversibly damage the cellular membrane. Fig. 2 shows

the molecular lipophilicity potential (MLP) map and polar surface areas (PSAs) of selected (*Z*)-2,3-diphenylacrylonitrile analogs. In the present study, compound **3c** was the most active, followed by compounds **3f**, **3i**, and **3h** with PSAs of 27.03, 23.792, 23.792, and 23.792, respectively. Although a small number of compounds were used in the present study, a good correlation was observed in which cytotoxic activity decreased with increasing PSA (Fig. 3). It is well known that PSA, *i.e.* polarity, is correlated with the lipophilicity of a molecule, which is an important factor for biological activity. The correlation coefficients (r^2) between the PSAs and inhibitory potencies of selected (*Z*)-2,3-diphenylacrylonitrile analogs against A549, human SK-OV-3, SK-MEL-2, and HCT15 cells were found to be 0.78 ($n = 11$), 0.83 ($n = 10$), 0.78 ($n = 11$), and 0.79 ($n = 13$), respectively. The above correlations should be treated with caution since there were three exceptions, *e.g.* PSAs of moderately active compounds **3a** (23.792) and **3g** (23.792) were the same as highly active compound **3f** (23.792), whereas PSA of active compound **3p** (69.616) was as high as similarly active compound **3h** (23.792). Therefore, maps of PSA and MLP were compared for compounds **3a**, **3f**, **3g**, **3h**, and **3p** (Fig. 2). It was found that polarity and lipophilicity were different for all molecules. On the other hand, compounds **3a**, **3f**, and **3g** showed similar PSAs, whereas compound **3f** showed a greater lipophilic area compared to that of compound **3a** or **3g**. Similarly, although the PSA of compound **3p** was higher than that of compound **3h**, their MLP maps were almost the same. The design and synthesis of additional (*Z*)-2,3-diphenylacrylonitrile analogs containing lipophilic and hydrophilic substituents are in progress in order to corroborate our findings.

2.4. Anti-microbial activity

The newly synthesized (*Z*)-2,3-diphenylacrylonitrile analogs (**3a**–**r**) were evaluated for their *in vitro* anti-bacterial activities

Table 3
In vitro anti-microbial profiles of (Z)-2,3-diphenylacrylonitrile analogs (**3a**–**r**) in terms of zone of inhibition.

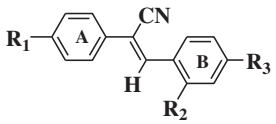

Comp	R_1	R_2	R_3	Inhibition zone in mm		
				S. aureus	*S. typhi*	*A. niger*
3a	H	H	H	–	7 ± 0.5	–
3b	H	H	OMe	–	10 ± 1.0	–
3c	H	H	NMe_2	–	10 ± 1.0	–
3d	H	NO_2	H	–	8 ± 0.5	–
3e	H	H	NO_2	–	7 ± 0.5	–
3f	H	H	Cl	–	10 ± 1.0	–
3g	H	Cl	H	–	8 ± 0.5	–
3h	H	H	Br	–	9 ± 0.5	–
3i	H	H	CH_3	–	11 ± 1.0	–
3j	NO_2	H	H	–	8 ± 0.5	–
3k	NO_2	H	OMe	18 ± 0.5	13 ± 1.0	–
3l	NO_2	H	NMe_2	12 ± 0.5	11 ± 0.5	–
3m	NO_2	NO_2	H	11 ± 0.5	7 ± 0.5	–
3n	NO_2	H	NO_2	11 ± 1.0	7 ± 0.5	–
3o	NO_2	H	Cl	–	9 ± 0.5	–
3p	NO_2	Cl	H	–	10 ± 1.0	–
3q	NO_2	H	Br	–	8 ± 0.5	–
3r	NO_2	H	CH_3	–	10 ± 1.0	–
Azithromycin				19 ± 1.0	21 ± 1.0	18 ± 1.0

Inhibitory activity is expressed as the diameter (in mm) of the observed inhibition zone. Data show means ± SD ($n = 3$). Concentration of each compound is 100 μg $disc^{-1}$, whereas that of positive control is 25 μg $disc^{-1}$.

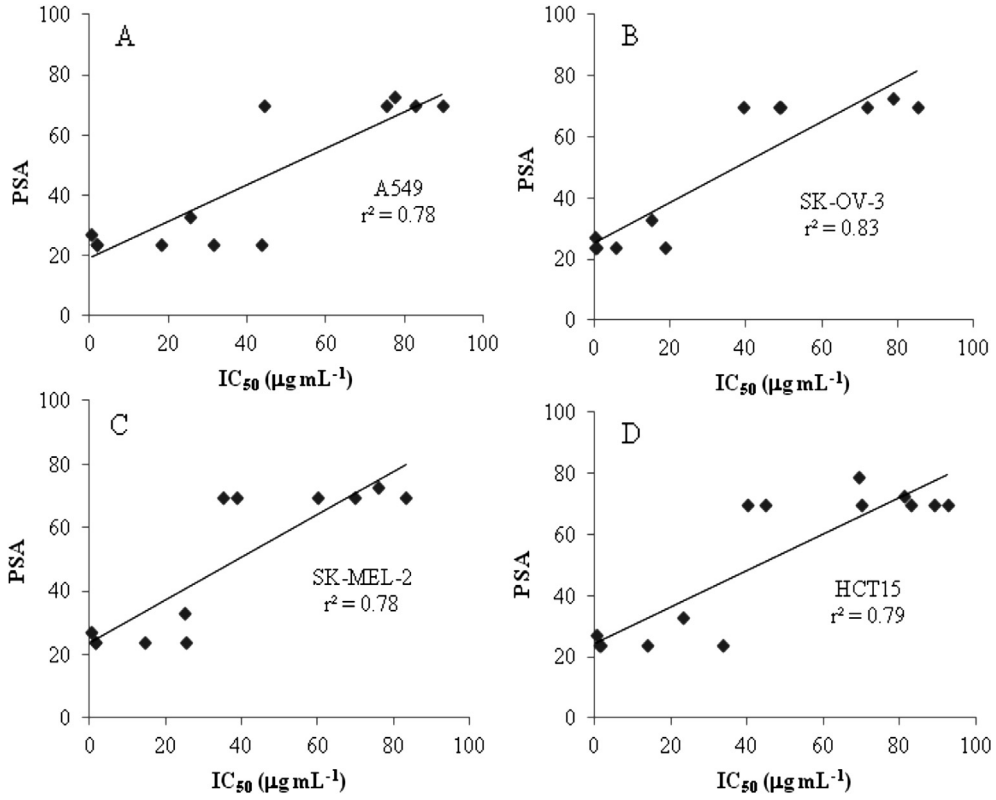

Fig. 3. Correlation between polar surface area (PSA) and inhibitory potency in selected (*Z*)-2,3-diphenylacrylonitrile analogs against (A) human lung cancer (A549), (B) human ovarian cancer (SK-OV-3), (C) human skin cancer (SK-MEL-2), and (D) human colon cancer (HCT15) cells.

against two bacterial strains, *e.g. S. aureus* (Gram-positive) and *S. typhi* (Gram-negative), as well as their anti-fungal activities against *A. niger* by the disc diffusion method. Results of the *in vitro* evaluation of anti-microbial activity are reported in Table 3. Inhibition zones of synthesized compounds were measured at doses of 100 mg disc^{-1}, and azithromycin as a positive control was evaluated at a dose of 25 mg disc^{-1}. As presented in Table 3, all compounds inhibited the growth of *S. typhi*, and compounds **3k**–**n** resisted both *S. aureus* and *S. typhi*. None of the compounds were significantly active against *A. niger* at a concentration of 100 mg disc^{-1}. Among all of them, compound **3k** showed the highest activities against both *S. aureus* and *S. typhi*, followed by compound **3l**. Compounds **3c**, **3f**, **3i**, **3k**, **3p**, and **3r** showed high activities against *S. typhi*, whereas compounds **3b**, **3d**, **3e**, **3g**, **3h**, **3j**, **3m**–**o**, and **3q** exhibited moderate activities against the same bacterial strain. At the same concentration, *i.e.* 100 mg disc^{-1}, compounds **3k**–**n** demonstrated greater activities against *S. aureus* compared to *S. typhi*. From this study, (*Z*)-2,3-diphenylacrylonitriles appeared to be more active against Gram-negative bacteria compared to Gram-positive bacteria.

Structure–activity relationships may be explained briefly as follows: introduction of an electron-withdrawing group (NO_2), a highly polar group, into the *para*-position of ring A of compounds **3a**–**i** yielded compounds **3j**–**r**, which showed slightly increased bactericidal activities against *S. typhi* in the case of compounds **3j**–**l**, **3p**, and **3r**, reduced activities in the case of compounds **3m**, **3o**, and **3q**, and no change in the case of compound **3n**. Introduction of this same polar group (NO_2) into the *para*-position of ring A of compounds **3b**–**e** yielded compounds **3k**–**n**, which showed good anti-bacterial activities against *S. aureus*, whereas compounds **3a**–**i**, and their *para*-nitro analogs (**3j** and **3o**–**r**) were inactive. Introduction of electron-donating groups (halogen, OMe, NMe_2, and CH_3) at the R_3 position resulted in increased activity (cf., **3b**, **3c**, **3f**, **3i**, **3k,** and **3l**), whereas the presence of an electron-withdrawing group (NO_2) caused a reduction in activity (cf., **3d**, **3e**, **3m**, and **3n**).

3. Conclusion

The present study reports the synthesis of novel (*Z*)-2,3-diphenylacrylonitrile analogs as well as their biological evaluation as cytotoxic and anti-bacterial agents. Using the Knoevenagel condensation reaction, 18 compounds were prepared and their cytotoxicities against four cancer cell lines, *e.g.* lung cancer (A549), ovarian cancer (SK-OV-3), skin cancer (SK-MEL-2), and colon cancer (HCT15), as well as anti-microbial activities against three microbes, *e.g. S. aureus*, *S. typhi*, and *A. niger*, evaluated. Compound **3c** showed the highest cytotoxic activities against all cancer cell lines, followed by compounds **3f**, **3i**, and **3h** containing *N*,*N*-dimethylamine, chloro, methyl, and bromo substituents at the *para*-position of the phenyl ring A, respectively. Compound **3c** exhibited 2.4 times greater cytotoxic activity against HCT15 cells, whereas it showed similar potency against SK-OV-3 cells to that of the standard anti-cancer agent doxorubicin. Introduction of electron-donating groups at the *para*-position of the phenyl ring B was favorable for improved cytotoxic activity, whereas the presence of an electron-withdrawing group was unfavorable compare to unsubstituted acrylonitrile. Physicochemical calculations indicate that the cytotoxicities of (*Z*)-2,3-diphenylacrylonitriles correlated well with the calculated PSA and MLP. Most of the compounds showed significant bactericidal activities against *S. typhi*, whereas compound **3k** showed potent activity against both *S. aureus* and *S. typhi*. The strong cytotoxicities of compounds **3c**, **3f**, **3i**, and **3h** combined with our computational results will be helpful in synthesizing a large library of (*Z*)-2,3-diphenylacrylonitrile analogs for extensive anti-cancer study as well as for the development of a more appropriate drug candidate.

4. Experimental

4.1. General

Melting points were determined on an X-5 melting point apparatus (Yuxiagyiqi, Gongyi City Yuxiang Instruments Co., Ltd., China) and are uncorrected. IR spectra were obtained with an FTIR-8430S (Shimadzu, Japan) using KBr discs. NMR spectra were recorded on a Unity INOVA 500 MHz NMR (Varian, USA) or an AM-400 MH (Bruker, USA) spectrometer using $CDCl_3$ or acetone-d_6 with TMS as an internal standard. Elemental analyses (C, H, N) were performed on a Perkin–Elmer 2400 II CHN elemental analyzer.

4.2. General procedure for preparation of 2,3-diphenylacrylonitrile analogs (*3a*–*r*)

Benzyl cyanide or substituted benzyl cyanides (2.0 mmol) were added to substituted benzaldehydes (2.5 mmol) in ethanol (15–20 mL), after which the mixture was stirred at room temperature for 10–15 min. To this solution, sodium ethoxide (0.7 g, 10 mmol) in the same solvent (10 mL) was added dropwise with constant stirring, and the reaction mixture was vigorously stirred for 20–72 h to complete the reaction, which was monitored by TLC. After removal of the solid materials and solvent, crude products were purified by silica gel column chromatography (eluent: mixtures of dichloromethane and *n*-hexane from 1:1 to 7:3 gradient).

4.2.1. (*Z*)-2,3-Diphenylacrylonitrile (*3a*) [33]

Yield 96%, mp 85–86 °C (white solids). IR (KBr) ν_{max}: 2218 cm^{-1} (CN). ^{1}H NMR spectrum: (400 MHz; $CDCl_3$) δ (ppm): 7.41 (m, 6H, Ar), 7.52 (brs, 1H, =CH), 7.66 (m, 2H, Ar), 7.87 (m, 2H, Ar). Anal. Calcd for $C_{15}H_{11}NC$ 87.77; H 5.40; N 6.82%. Found C 87.70; H 5.38; N 6.87%.

4.2.2. (*Z*)-3-(4-Methoxyphenyl)-2-phenylacrylonitrile (*3b*) [34]

Yield 81%, mp 93–94 °C (yellow solids). IR (KBr) ν_{max}: 2208 cm^{-1} (CN). ^{1}H NMR spectrum: (400 MHz; $CDCl_3$) δ (ppm): 3.87 (s, 3H, OCH_3), 6.98 (m, 2H, Ar), 7.39 (m, 3H, Ar), 7.16 (brs, 1H, =CH), 7.65 (m, 2H, Ar), 7.88 (m, 2H, Ar). Anal. Calcd for $C_{16}H_{13}NO$ C 81.68; H 5.57; N 5.95%. Found C 81.57; H 5.52; N 6.02%.

4.2.3. (*Z*)-3-(4-(Dimethylamino)phenyl)-2-phenylacrylonitrile (*3c*)

Yield 94%, mp 101–102 °C (pale yellow solids). IR (KBr) ν_{max}: 2210 cm^{-1} (CN). ^{1}H NMR spectrum: (400 MHz; $CDCl_3$) δ (ppm): 2.91 (s, 6H, $-N(CH_3)_2$), 7.01 (m, 2H, Ar), 7.38 (m, 3H, Ar), 7.49 (brs, 1H, =CH), 7.67 (m, 2H, Ar), 7.85 (m, 2H, Ar). Anal. Calcd for $C_{17}H_{16}N_2$ C 82.22; H 6.49; N 11.28%. Found C 82.17; H 6.45; N 11.36%.

4.2.4. (*Z*)-3-(2-Nitrophenyl)-2-phenylacrylonitrile (*3d*)

Yield 95%, mp 106–107 °C (white solids). IR (KBr) ν_{max}: 2218 cm^{-1} (CN). ^{1}H NMR spectrum: (400 MHz; $CDCl_3$) δ (ppm): 7.36 (m, 3H, Ar), 7.58 (m, 2H, Ar), 6.99 (brs, 1H, =CH), 7.83 (m,2H, Ar), 7.94 (m, 1H, Ar). Anal. Calcd for $C_{15}H_{10}N_2O_2$ C 71.99; H 4.03; N 11.19%. Found C 71.91; H 3.98; N 11.26%.

4.2.5. (*Z*)-3-(4-Nitrophenyl)-2-phenylacrylonitrile (*3e*)

Yield 94%, .p 110–112 °C (yellow solids). IR (KBr) ν_{max}: 2220 cm^{-1} (CN). ^{1}H NMR spectrum: (400 MHz; acetone-d_6) δ (ppm): 7.41 (m, 3H, Ar), 7.08 (brs, 1H, =CH), 7.68 (m, 2H, Ar), 7.81 (m, 2H, Ar), 7.96 (m, 2H, Ar). Anal. Calcd for $C_{15}H_{10}N_2O_2$ C 71.99; H 4.03; N 11.19%. Found C 71.93; H 3.97; N 11.25%.

*4.2.6. (Z)-3-(4-Chlorophenyl)-2-phenylacrylonitrile (**3f**)*

Yield 96%, mp 103–104 °C (white solids). IR (KBr) ν_{max}: 2205 cm^{-1} (CN). ^1H NMR spectrum: (400 MHz; $CDCl_3$) δ (ppm): 7.11 (m, 2H, Ar), 7.42 (m, 3H, Ar), 7.51 (brs, 1H, =CH), 7.67 (m, 2H, Ar), 7.86 (m, 2H, Ar). Anal. Calcd for $C_{15}H_{10}ClN$ C 75.16; H 4.21; N 5.84%. Found C 75.11; H 4.18; N 5.89%.

*4.2.7. (Z)-3-(2-Chlorophenyl)-2-phenylacrylonitrile (**3g**)*

Yield 92%, mp 97–98 °C (white solids). IR (KBr) ν_{max}: 2230 cm^{-1} (CN). ^1H NMR spectrum: (400 MHz; $CDCl_3$) δ (ppm): 7.19 (m, 3H, ArH), 7.48 (m, 3H, ArH), 7.29 (brs, 1H, =CH), 7.79 (m, 3H, ArH). Anal. Calcd for $C_{15}H_{10}ClN$: C 75.16, H 4.21, N 5.84. Found: C 75.10, H 4.19, N 5.90.

*4.2.8. (Z)-3-(4-Bromophenyl)-2-phenylacrylonitrile (**3h**)*

Yield 95%, mp 89–90 °C (white solids). IR (KBr) ν_{max}: 2190 cm^{-1} (CN). ^1H NMR spectrum: (400 MHz; $CDCl_3$) δ (ppm): 7.07 (m, 2H, Ar), 7.34 (m, 3H, Ar), 7.47 (brs, 1H, =CH), 7.58 (m, 2H, Ar), 7.69 (m, 2H, Ar). Anal. Calcd for $C_{15}H_{10}BrN$ C 63.40; H 3.55; N 4.93%. Found C 63.37; H 3.51; N 4.99%.

*4.2.9. (Z)-2-Phenyl-3-P-tolylacrylonitrile (**3i**) [30]*

Yield 85%, mp 61–62 °C (white solids). IR (KBr) ν_{max}: 2213 cm^{-1} (CN). ^1H NMR spectrum: (400 MHz; $CDCl_3$) δ (ppm): 2.41 (s, 3H, CH_3), 7.27 (m, 2H, Ar), 7.41 (m, 3H, Ar), 7.50 (brs, 1H, =CH), 7.67 (m, 2H, Ar), 7.80 (m, 2H, Ar). Anal. Calcd for $C_{16}H_{13}N$ C 87.64; H 5.98; N 6.39%. Found C 87.53; H 5.86; N 6.42%.

*4.2.10. (Z)-2-(4-Nitrophenyl)-3-phenylacrylonitrile (**3j**)*

Yield 91%, mp 143–142 °C (red solids). IR (KBr) ν_{max}: 2220 cm^{-1} (CN). ^1H NMR spectrum: (400 MHz; $CDCl_3$) δ (ppm): 7.31 (m, 3H, Ar), 7.51 (m, 2H, Ar), 7.11 (brs, 1H, =CH), 7.79 (m, 2H, Ar), 7.94 (m, 2H, Ar). Anal. Calcd for $C_{15}H_{10}N_2O_2$ C 71.99; H 4.03; N 11.19%. Found C 71.95; H 4.00; N 11.23%.

*4.2.11. (Z)-3-(4-Methoxyphenyl)-2-(4-nitrophenyl)acrylonitrile (**3k**)*

Yield 92%, mp 109–110 °C (pale red solids). IR (KBr) ν_{max}: 2201 cm^{-1} (CN). ^1H NMR spectrum: (400 MHz; $CDCl_3$) δ (ppm): 3.89 (s, 3H, OCH_3), 6.97 (m, 2H, Ar), 7.41 (m, 2H, Ar), 7.08 (brs, 1H, =CH), 7.79 (m, 2H, Ar), 7.91 (m, 2H, Ar). Anal. Calcd for $C_{16}H_{12}N_2O_3$ C 68.56; H 4.32; N 9.99%. Found C 68.49; H 4.29; N 10.02%.

*4.2.12. (Z)-3-(4-(Dimethylamino)phenyl)-2-(4-nitrophenyl) acrylonitrile (**3l**)*

Yield 89%, mp 114–115 °C (deep red solids). IR (KBr) ν_{max}: 2208 cm^{-1} (CN). ^1H NMR spectrum: (400 MHz; $CDCl_3$) δ (ppm): 2.89 (s, 6H, $-N(CH_3)_2$), 6.89 (m, 2H, Ar), 7.33 (m, 2H, Ar), 7.48 (brs, 1H, =CH), 7.71 (m, 2H, Ar), 7.89 (m, 2H, Ar); Anal. Calcd for $C_{17}H_{15}N_3O_2$ C 69.61; H 5.15; N 14.33%. Found C 69.58; H 5.11; N 14.37%.

*4.2.13. (Z)-3-(2-Nitrophenyl)-2-(4-nitrophenyl)acrylonitrile (**3m**)*

Yield 92%, mp 161–162 (yellowish red solids). IR (KBr) ν_{max}: 2222 cm^{-1} (CN). ^1H NMR spectrum: (400 MHz; $CDCl_3$) δ (ppm): 7.46 (m, 1H, Ar), 6.96 (brs, 1H, =CH), 7.91 (m, 4H, Ar), 8.07 (m, 3H, Ar). Anal. Calcd for $C_{15}H_9N_3O_4$ C 61.02; H 3.07; N 14.23%. Found C 60.96; H 3.02; N 14.27%.

*4.2.14. (Z)-2,3-Bis(4-nitrophenyl)acrylonitrile (**3n**)*

Yield 94%, mp 156–157 °C (pale red solids). IR (KBr) ν_{max}: 2230 cm^{-1} (CN). ^1H NMR spectrum: (400 MHz; $CDCl_3$) δ (ppm): 6.96 (brs, 1H, =CH), 7.89 (m, 4H, Ar), 8.02 (m, 4H, Ar); Anal. Calcd for $C_{15}H_9N_3O_4$ C 61.02; H 3.07; N 14.23%. Found C 60.98; H 3.03; N 14.28%.

*4.2.15. (Z)-3-(4-Chlorophenyl)-2-(4-nitrophenyl)acrylonitrile (**3o**)*

Yield 87%, mp 139–140 °C (yellowish red solids). IR (KBr) ν_{max}: 2199 cm^{-1} (CN). ^1H NMR spectrum: (400 MHz; $CDCl_3$) δ (ppm): 7.39 (m, 2H, Ar), 7.52 (m, 2H, Ar), 7.19 (brs, 1H, =CH), 7.81 (m, 2H, Ar), 7.97 (m, 2H, Ar). Anal. Calcd for $C_{15}H_9ClN_2O_2$ C 63.28; H 3.19; N 9.84%. Found C 63.24; H 3.16; N 9.87%.

*4.2.16. (Z)-3-(2-Chlorophenyl)-2-(4-nitrophenyl)acrylonitrile (**3p**)*

Yield 92%, mp 124–126 °C (yellowish red solids). IR (KBr) ν_{max}: 2226 cm^{-1} (CN). ^1H NMR spectrum: (400 MHz; $CDCl_3$) δ (ppm): 7.11 (m, 2H, Ar), 7.46 (m, 2H, Ar), 7.13 (brs, 1H, =CH), 7.78 (m, 2H, Ar), 8.03 (m, 2H, Ar); Anal. Calcd for $C_{15}H_9ClN_2O_2$ C 63.28; H 3.19; N 9.84%. Found C 63.25; H 3.15; N 9.88%.

*4.2.17. (Z)-3-(4-Bromophenyl)-2-(4-nitrophenyl)acrylonitrile (**3q**)*

Yield 95%, mp 128–130 °C (yellowish red solids). IR (KBr) ν_{max}: 2220 cm^{-1} (CN). ^1H NMR spectrum: (400 MHz; $CDCl_3$) δ (ppm): 7.43 (m, 2H, Ar), 7.15 (brs, 1H, =CH), 7.64 (m, 2H, Ar), 7.82 (m, 2H, Ar), 7.99 (m, 2H, Ar); Anal. Calcd for $C_{15}H_9BrN_2O_2$ C 54.74; H 2.76; N 8.51%. Found C 54.69; H 2.71; N 8.55%.

*4.2.18. (Z)-2-(4-Nitrophenyl)-3-p-tolylacrylonitrile (**3r**)*

Yield 91%, mp 13–132 °C (pale yellow solids). IR IR (KBr) ν_{max}: 2215 cm^{-1} (CN). ^1H NMR spectrum: (400 MHz; $CDCl_3$) δ (ppm): 2.42 (s, 3H, CH_3), 7.17 (m, 2H, Ar), 7.40 (m, 2H, Ar), 7.09 (brs, 1H, =CH), 7.87 (m, 2H, Ar), 8.01 (m, 2H, Ar). Anal. Calcd for $C_{16}H_{12}N_2O_2$ C 72.72; H 4.58; N 10.60%. Found C 72.68; H 4.55; N 10.66%.

4.3. Biological assay

4.3.1. Cytotoxicity assay

Cytotoxicity after treatment of tumor cells with the test materials was determined using the SRB (sulforhodamine-B) method, currently adopted in the NCI's *in vitro* anti-cancer drug screening [35], *i.e.* the inhibition rate of cell proliferation was estimated after continuous exposure to the test materials for 48 h. All samples were tested in triplicate, and the mean IC_{50} values (mg/mL) (concentration of compound resulting in 50% inhibition of cell proliferation) and S.E.M. were calculated.

4.3.2. Anti-bacterial screening

A previously described filter paper disc diffusion method [36] against two strains was used for determination of the *in vitro* anti-bacterial effects of all samples. Briefly, nutrient agar (NA) media (Difco laboratories, Lawrence, KS) was used as a basal medium for test bacteria. These agar media were inoculated with 0.2 mL of the 24-h liquid cultures containing the microorganisms. The sample discs were placed gently on pre-inoculated agar plates and then incubated aerobically at 37 °C for 24 h. Discs with only DMSO were used as a control, and azithromycin was used as a positive control. Inhibitory activity was measured (in mm) as the diameter of the observed inhibition zones. These evaluations were performed in triplicate for each compound at a concentration of 100 μg $disc^{-1}$.

4.3.3. Anti-fungal screening

Using the standard disc diffusion method [36], all samples were tested *in vitro* for their anti-fungal properties against *A. niger*. Briefly, potato dextrose agar (Difco) was used as a basal medium for testing of fungi. Sterilized melted PDA medium (~45 °C) was poured into a Petri dish (90 mm) and solidified. Prepared discs of samples were placed gently on solidified agar plates and freshly seeded with the test organisms using sterile forceps. Discs with DMSO and azithromycin were used as negative and positive controls, respectively. Plates were incubated at 30±1 °C for 72 h. DMSO

was used as a solvent for preparation of desired solutions of the test samples.

4.4. Computational methods

The molecular geometries of the (*Z*)-2,3-diphenylacrylonitrile analogs were built with a standard bond length and angles using the ChemBio3D ultra Ver. 12 molecular modeling program (CambridgeSoft Corporation, Cambridge, MA 02140 USA). The energy was minimized by the semi-empirical molecular orbital PM3 method [37]. Physicochemical properties were calculated using molinspiration cheminformatics software (Molinspiration Cheminformatics, SK 90026 Slovensky Grob, SR). The method for calculation of clogP was developed by Molinspiration (miLogP2.2–2005) based on group contributions and correction factors by fitting calculated log P with experimental log P for a training set more than twelve thousand, mostly drug-like molecules. Molecular polar surface area (PSA) was calculated based on the methodology published by Ertl et al. [38] as a sum of fragment contributions. The maps of molecular lipophilicity potential (MLP) and polar surface area (PSA) were viewed in Molinspiration Galaxy 3D Structure Generator (ver. 2010.02 beta) using an optimized structure generated by the semi-empirical molecular orbital PM3 method.

Acknowledgments

Dr. Seen Ae Chae at Korea Basic Science Institute (Daegu) is acknowledged for the NMR data.

Appendix A. Supplementary data

Supplementary data related to this article can be found at http://dx.doi.org/10.1016/j.ejmech.2013.08.031.

References

[1] T.M. Tagmose, F. Zaragoza, H.C.M. Boonen, A. Worsaae, J.P. Mogensen, F.E. Nielsen, A.F. Jensen, J.B. Hansen, Bioorg. Med. Chem. 11 (2003) 931–940.
[2] A. Carta, P. Sanna, M. Palomba, L. Vargiu, M. La Colla, R. Loddo, Eur. J. Med. Chem. 37 (2002) 891–900.
[3] P. Sanna, A. Carta, M.E. Rahbar Nikookar, Eur. J. Med. Chem. 35 (2000) 535–543.
[4] P. Sanna, A. Carta, L. Gherardini, M.E. Rahbar Nikookar, Farmaco 57 (2002) 79–87.
[5] F. Sączewski, P. Reszka, M. Gdaniec, R. Grünert, P.J. Bednarski, J. Med. Chem. 47 (2004) 3438–3449.
[6] F. Sączewski, A. Stencel, A.M. Bieńczak, K.A. Langowska, M. Michaelis, W. Werel, R. Hałasa, P. Reszka, P.J. Bednarski, Eur. J. Med. Chem. 43 (2008) 1847–1857.
[7] M. Hranjec, G. Pavlović, M. Marjanović, M. Kralj, G. Karminski-Zamola, Eur. J. Med. Chem. 45 (2010) 2405–2417.
[8] C.A. Zificsak, Y. Shen, J.G. Lisko, J.P. Theroff, X. Lao, O. Bollt, X. Li, B.D. Dorsey, S.K. Kuwada, Bioorg. Med. Chem. Lett. 22 (2012) 1850–1853.
[9] B.B. Aggarwal, A. Bhardwaj, R.S. Aggarwal, N.P. Seeram, S. Shishodia, Y. Takada, Anticancer Res. 24 (2004) 2783–2840.
[10] M. Jang, L. Cai, G.O. Udeani, K.V. Slowing, C.F. Thomas, C.W. Beecher, H.H. Fong, N.R. Farnsworth, A.D. Kinghorn, R.G. Mehta, R.C. Moon, J.M. Pezzuto, Science 275 (1997) 218–220.
[11] P. Signorelli, R.J. Ghidoni, J. Nutr. Biochem. 16 (2005) 449–466.
[12] S.H. Inayat-Hussain, N.F. Thomas, Expert Opin. Ther. Pat. 14 (2004) 819–835.
[13] C. Lion, C.S. Matthews, M.F.G. Stevens, A.D. Westwell, J. Med. Chem. 48 (2005) 1292–1295.
[14] F. Minutolo, G. Sala, A. Bagnacani, S. Bertini, I. Carboni, G. Placanica, G. Prota, S. Rapposelli, N. Sacchi, M. Macchia, R. Ghidoni, J. Med. Chem. 48 (2005) 6783–6786.
[15] M. Gao, M. Wang, K.D. Miller, G.W. Sledge, G.D. Hutchins, Q.-H. Zheng, Bioorg. Med. Chem. Lett. 16 (2006) 5767–5772.
[16] M.C. Hong, Y.K. Kim, J.Y. Choi, S.Q. Yang, H. Rhee, Y.H. Ryu, T.H. Choi, G.J. Cheon, G.I. An, H.Y. Kim, Y. Kim, D.J. Kim, J.-S. Lee, Y.-T. Chang, K.C. Lee, Bioorg. Med. Chem. 18 (2010) 7724–7730.
[17] L.A. Stivala, M. Savio, F. Carafoli, P. Perucca, L. Bianchi, G. Maga, L. Forti, U.M. Pagoni, A. Albini, E. Prosperi, V. Vannini, J. Biol. Chem. 276 (2001) 22586–22594.
[18] Y. Kimura, H. Okuda, S. Arichi, Biochim. Biophys. Acta 834 (1985) 275–278.
[19] F. Scarlatti, G. Sala, G. Somenzi, P. Signorelli, N. Sacchi, R. Ghidoni, FASEB J. 17 (2003) 2339–2341.
[20] G. Sala, F. Minutolo, M. Macchia, N. Sacchi, R. Ghidoni, Drugs Exp. Clin. Res. 29 (2003) 263–269.
[21] B. Ogretmen, Y. Hannun, Nat. Rev. Cancer 4 (2004) 604–616.
[22] C. Patrick Reynolds, B. Maurer, R.N. Kolesnick, Cancer Lett. 206 (2004) 169–180.
[23] M. Selzner, A. Bielawska, A.M. Morse, H.A. Rudiger, D. Sindram, Y.A. Hannun, P.A. Clavien, Cancer Res. 61 (2001) 1233–1240.
[24] P. de Medina, R. Casper, J.-F. Savouret, M. Poirot, J. Med. Chem. 48 (2005) 287–291.
[25] M. Roberti, D. Pizzirani, D. Simoni, R. Rondanin, R. Baruchello, C. Bonora, F. Buscemi, S. Grimaudo, M. Tolomeo, J. Med. Chem. 46 (2003) 3546–3554.
[26] S. Kim, H. Ko, J.E. Park, S. Jung, S.K. Lee, Y.-J. Chun, J. Med. Chem. 45 (2002) 160–164.
[27] A. Levitzki, E. Mishani, Annu. Rev. Biochem. 75 (2006) 93–109.
[28] A.M. Alafeefy, S.I. Alqasoumi, A.E. Ashour, V. Masand, N.A. Al-Jaber, T. Ben Hadda, M.A. Mohamed, Eur. J. Med. Chem. 53 (2012) 133–140.
[29] G. Wells, A. Seaton, M.F.G. Stevens, J. Med. Chem. 43 (2000) 1550–1562.
[30] I. Esen, C. Yolacan, F. Aydogan, Bull. Korean Chem. Soc. 31 (2010) 2289–2292.
[31] L. Türkeer, E. Sener, I. Yalçín, U. Akbulut, I. Kayalidere, Sci. Pharm. 58 (1990) 107–113.
[32] B. Testa, P.-A. Carrupt, P. Gaillard, F. Billois, Pharm. Res. 13 (1996) 335–343.
[33] D. Villemin, A. Jullien, N. Bar, Green Chem. 5 (2003) 467–469.
[34] A. Loupy, M. Pellet, A. Petit, G. Vo-Thanh, Org. Biomol. Chem. 3 (2005) 1534–1540.
[35] P. Skehan, R. Streng, D. Scudiero, A. Monks, J. McMahon, D. Vistica, J.T. Warren, H. Bokesch, S. Kenney, M.R. Boyd, J. Natl. Cancer Inst. 82 (1990) 1107–1112.
[36] M.S. Alam, L. Liu, Y.E. Lee, D.U. Lee, Chem. Pharm. Bull. 59 (2011) 568–573.
[37] J.J.P. Stewart, J. Mol. Model 10 (2004) 155–164.
[38] P. Ertl, B. Rohde, P. Selzer, J. Med. Chem. 43 (2000) 3714–3717.